Electroelastic Coupling between Membrane-Embedded Charges and Membrane Fluctuations: Continuum Multi-Dielectric Treatment

Michael B. Partenskii, Gennady V. Miloshevsky and Peter C. Jordan
Department of Chemistry, Brandeis University, Waltham, MA, USA

Abstract

There is growing interest in understanding effects due to electrostatically promoted membrane-water fluctuations, which may influence voltage gating in proteins. Membrane geometry is significantly altered by electrostatic interactions with membrane-embedded charges. We use a modified continuum model to study the interactions of a charge with surface fluctuations for arbitrarily shaped membrane-water interfaces in multi-dielectric environments. We surround a point charge by a sphere of low dielectric constant and solve the linear Poisson-Boltzmann equation, directly calculating the potential due to the reaction field via a method that eliminates self-energy contributions. This permits treating a charge in a mixed lipid/water environment, e.g. one crossing the fluctuating membrane-water interface or interacting with a water plume penetrating the membrane's hydrophobic core. We determine the energetics and optimized shapes of such aqueous deformations interacting electroelastically with the charge located at various positions in the membrane.

Introduction

Electroelastic coupling of electric fields or charges to membrane fluctuations is important for membrane stability, electroporation, ionic transport and voltage gating [1]. This issue became especially relevant due to the break-through discovery [2] that the gating charges in some voltage gated-channels are partially embedded in lipid bilayers, which raises a question of possible stabilizational mechanisms in low-dielectric media.

We study coupling of membrane fluctuations to a single charge bound within the membrane. We use the elastic "smectic bilayer" model of the membrane and demonstrate that the charge's solvation energy is bistable: at some charge value, there is a new low-energy state with the charge solvated by a water "dimple". The corresponding membrane deformations, however, typically exceed the applicability range of the linear smectic model. This prompted analysis of another route of instability, one where elastic fluctuations trigger massive water penetration into the membrane's hydrophobic core. We use kMC reaction path following [3] of the water dimple and the charge across the membrane to find energy minima and to determine the energy profiles along the reaction pathways.

Computational Model

Source-free Poisson-Boltzmann equation, $\phi_\delta = \phi - \phi_c$

$\nabla \cdot \varepsilon \nabla \phi_\delta = -\nabla \cdot (\varepsilon - \varepsilon_p) \nabla \phi_c$ where $\phi_\delta = \phi - \phi_c$, ε_p - dielectric constant near the charge, ϕ_c - the coulombic potential calculated analytically from $\varepsilon_p \nabla^2 \phi_c = -4\pi q$ [4].

Inside the charge sphere $\varepsilon = \varepsilon_p = 1$, the Poisson-Boltzmann equation is $\varepsilon_p \nabla^2 \phi_\delta = 0$

Outside the charge sphere ϕ_c is well defined; thus

- singularities due to point charges are eliminated
- reaction field potentials are computed directly

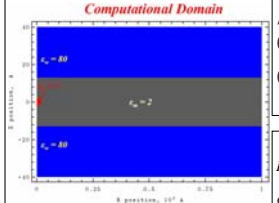

Cylindrical geometry: r = 0 ÷ 100 Å; z = -40 ÷ 40 Å; mesh step: 0.1 Å; 1001 × 801 grid points

Boundary Conditions

$\phi_\delta = \phi - \phi_c = 0 - \dfrac{q}{\varepsilon_p \rho(r_b, z_b)}$, where

$\rho(r_b, z_b) = \sqrt{(r_b - r_0)^2 + (z_b - z_0)^2}$

(r_0, z_0) - the r and z coordinates of the point charge

(r_b, z_b) - the r and z coordinates of the boundary points in the computational domain

Electrostatic Energy

$E_{elect} = \dfrac{1}{2} q \phi_\delta(r_0, z_0)$, with

$\phi_\delta(r_0, z_0)$ - the potential of the reaction field at location of the point charge

Elastic Energy

$E_{elast} = 2\pi \int_0^R w(r) r dr$, where $w(r) = a(z_1(r) + z_2(r))^2 + b\left(LU_1(r)^2 + LU_2(r)^2\right)$ with $a = E_s / (2h^2)$ and $b = K_c / 4$. For DOPC: $E_s = 0.45\ kT/Å$, $K_c = 4.83\ kT$ and $h = 26\ Å$

For DMPC: $E_s = 0.35\ kT/Å$, $K_c = 13.5 \div 26.6\ kT$ and $h = 25.2\ Å$ (both for 300 K)

Gaussian Shape	Hertzian Shape
$z_i(r) = u_i \exp(-r^2/\lambda_i^2)$	$z_i(r) = u_i Kei(r/\lambda_i)/Kei(0)$
$LU_i(r) = -4u_i(\lambda_i^2 - r^2)\exp(-r^2/\lambda_i^2)/\lambda_i^4$	$LU_i(r) = u_i Ker(r/\lambda_i)/(\lambda_i^2 Kei(0))$ $\quad i = 1,2$

Solution Method

- MUltifrontal Massively Parallel Solver (MUMPS) [5], an accurate direct method based on *LU* matrix factorization, is used to solve the system of linear equations, **Ax** = **b**, where **A** is an unsymmetric sparse matrix. It utilizes MPI for message passing and makes use of the BLAS, BLACS and ScaLAPACK libraries.
- Continuum Electroelastics of Membrane Electrolyte Assembly (CE-MEA) parallel code is developed in mixed Fortran 90/95 and C/C++. It is implemented by using the MPI-2 standard for parallel communications. The CE-MEA code runs on a PC Linux or Windows Intel Cluster with 64 bit addressing.

kMC Reaction Path Following (kMCRPF)

kMCRPF [2] navigates on the energy surface, establishing minimum energy pathways and energy profiles

- Establish a system degree of freedom that can be identified as a reaction coordinate:

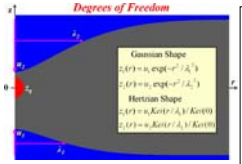

u_1, u_2 and λ_1, λ_2 are the amplitudes and decay lengths of the lower and upper water dimples; z_q is the charge's z-coordinate

- Force only unidirectional (constrained) motion along a reaction coordinate, all other degrees of freedom are unconstrained :

1. calculate the initial energy, E^{old}, of the system
2. perform a unidirectional move along the reaction coordinate
3. calculate the energy, E^{new}, of a new state and $\Delta E = E^{new} - E^{old}$
4. if $\Delta E \le 0$, accept a trial move; if $\Delta E > 0$, accept a trial move if $R \le \exp(-\Delta E/kT)$, where R is a random number between 0 and 1; otherwise reject it, reduce the maximum step length along the reaction coordinate and go to step 2
5. use the unconstrained Metropolis MC method to perform many MC trials relaxing the other degrees of freedom while fixing a reaction coordinate; go to step 2

- u_1 or u_2 can be used as a constrained degree of freedom; the charge can be fixed at various positions z_q along the z axis.
- z_q can be used as a reaction coordinate; then u_1, u_2, λ_1 and λ_2 are unconstrained degrees of freedom.

kMC Reaction Path Following of Water Dimple across the DOPC Membrane

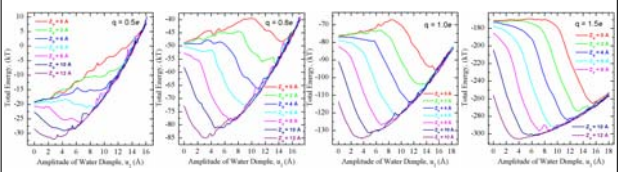

Figure 1. Total energy profiles as functions of the amplitude of a water dimple crossing a DOPC membrane (h = 26 Å). Profiles are plotted separately for different charge values, q. Each illustrates energies of a point charge bound to the membrane at $r_q = 0$ Å as a function of z_q. The charge is surrounded by a sphere of radius 2 Å and dielectric constant 1. Membrane and water regions' dielectric constants are 2 and 80 respectively. Water dimples are Hertzian in shape. In the spirit of kMCRPF [3], the amplitude u_2 (the reaction coordinate) was unidirectionally constrained to increase while the other degrees of freedom, u_1, λ_1 and λ_2, were freely variable (see movies [6]).

Main observations:

- Charges (0.5e < q < 1.5e) bound at $|z_q| > 4$ Å trigger significant thickness fluctuation resulting in their solvation by a water dimple (lower four curves). Membrane breakdown exacts no energetic cost. For positions nearer the center (upper three curves), stability depends strongly on q. For q = 0.5e, there is no stable state where the water dimple solvates the charge; energy increases steadily. At larger q, the system exhibits bistability. Consider the red curves corresponding to $|z_q| = 0$ Å. The activation barrier for dimple-solvated state formation changes from ~10 kT to ~0 kT as q varies from 0.8e to 1.5e. The stability of the solvated state relative to the unperturbed membrane also changes dramatically with q, with free energy difference varying from ~0 for q = 0.8e to ~ 95 kT (in favor of the dimple-solvated state) for q = 1.5e. The depth of the energy well corresponding to the dimple-solvated state increases and then decreases as the charge approaches the membrane surface. For example, for q = 1.0e

z_q, Å	0	2	4	6	8	10	12
ΔE, kT	20	28	37	43	45	41	21

- For $u_2 = 0$ Å (the corresponding $u_1 = 0$ and the membrane is practically unperturbed), the total energy drops as the charge approaches the surface. The minimum energy conformation describes an unperturbed membrane with the charge located in bulk water. All other conformations are of higher energy.
- When the dimple reaches the charge and solvates it, further rupture of the membrane is determined entirely by the elastic energy component.

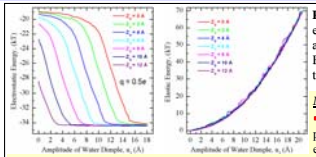

Figure 2. Profiles of the electrostatic and elastic energy as a function of the water dimple amplitude. Electrostatic profiles depict q = 0.5e. Energy profiles correspond to the charge bound to the membrane at $r_q = 0$ Å and various z_q.

Main observations:

- The shape and behavior of electrostatic energy profiles are the same for all charges. The largest energy drop ~15 kT (q = 0.5e) becomes ~60 kT (q = 1.0e), i.e. it changes by a factor of 4. For a charge bound at $|z_q| < 4$ Å, the electrostatic energy decreases slowly and then drops abruptly. For a charge bound at $|z_q| > 4$ Å, the electrostatic energy always drops sharply. The electrostatic energy doesn't change when the charge is solvated by the water dimple.
- For the unperturbed membrane ($u_2 = 0$ Å), the energy drops as the charge nears the membrane surface.
- As the water dimple penetrates the membrane, the elastic energy steadily increases, independently of the location of the charge or of its value.

kMC Reaction Path Following of the Charge across the DOPC Membrane

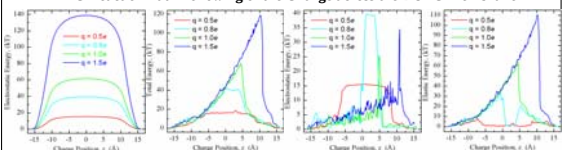

Figure 3. Dependence of total, electrostatic and elastic energy profiles on charge position for DOPC. For all q, electrostatic and total energies are differences, with reference states the unperturbed membrane with the charge immobilized in bulk water (z_q = -16 Å). The first plot portrays electrostatic energy profiles for a flat membrane (no water dimples). The other plots are energy profiles for membranes free to relax in response to charge motion for various q. The charge was unidirectionally constrained to cross the membrane using kMCRPF, with its axial position, z_q, the reaction coordinate (see movies [6]). Other degrees of freedom, u_1, λ_1, u_2 and λ_2, were freely variable. Higher q asymmetries may reflect insufficiently relaxed free variables.

Main observations:

- For q = 0.5e the water dimple disappears between z_q ~7 Å and ~7 Å. In this interior region the membrane is essentially unperturbed, the energy barrier (~15 kT) is electrostatics dominated and there is no dimple-aided solvation. Fig. 1 also shows that "dimple-solvated" states for q = 0.5e at $|z_q| < 5$ Å are energetically unfavorable relative to the conformation with the membrane unperturbed and the charge bound at $z_q = 0$ Å. For q = 0.8e dimple disappearance occurs between z_q ~0 Å and ~5 Å, where the charge is membrane exposed and electrostatics governs the barrier (~40 kT).
- For q > 0.8e the charge is always solvated by one of the water dimples. The interdimple switch occurs where solvation to the second dimple becomes energetically favorable. The energy barrier is dominated by the elastic component, which steadily increases (to ~60 and ~110 kT, q = 1.0e and 1.5e, respectively) and drops thereafter. The electrostatic energy fluctuates and increases (to ~5 and ~10 kT, q = 1.0e and 1.5e, respectively); its energy peak corresponds to the locus of the interdimple switch.

Water-filled Cylindrical Pore in the Membrane

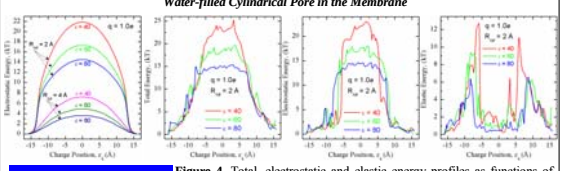

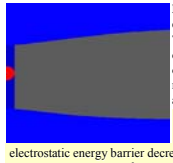

Figure 4. Total, electrostatic and elastic energy profiles as functions of charge position in a DOPC membrane with a cylindrical water-filled pore. The first plot portrays electrostatic energies for a flat membrane with pores of different radii (2 and 4 Å) and dielectric constants (40, 60 and 80). The other plots illustrate energy profiles for a membrane relaxing freely in response to charge motion along the pore. The pore's radius, R_{cyl}, is 2 Å and q = 1.0e. Dielectric constants of 40, 60 and 80 are contrasted.

Main observations:

- For a flat membrane with a water-filled cylindrical pore (Fig. 4), the electrostatic energy barrier decrease is 3 to 4 times that with no aqueous pore (Fig. 3). Upon increasing the pore radius from 2 to 4 Å, the energy barrier drops by a factor of 3 to 5.
- Regardless of pore ε, the membrane surface distorts and a water dimple forms as the charge enters the pore. As the charge translocates, the dimple first disappears and then reforms as the charge nears the pore exit (see movies [6]). This reflects strong screening of the charge by pore water.
- The energy barrier (~15-20 kT) is dominated by electrostatics. The elastic energy increases at the pore entrances due to membrane deformation and fluctuates near zero in the region between ~-7 and ~7 Å. At lower pore ε the membrane deformation is larger.

Conclusions

- Membrane fluctuations play important roles in stabilizing membrane-bound charges. In DOPC charges bound far from the midplane ($|z_q| > 4$ Å) always promoted significant thickness fluctuations, and were solvated by water dimples (Fig. 1). Closer to the membrane center, a larger charge is required for "breakdown." For a charge residing midplane, this "critical" value is ~ 0.8e.
- The shape of the transmembrane transition energy barrier is strongly affected by fluctuations and differs significantly from the classical picture, a planar (unperturbed) membrane. The optimized barrier shape alters from a "wide-bell" to a "triangular" shape (Fig. 3). Similar behavior was observed in fully atomistic MD simulations of a charged arginine side chain dragged across a lipid bilayer [7]. The real barrier is presumed symmetric relative to the midlpane. We think that asymmetry with ionic position chosen as the "reaction coordinate" reflects insufficient sampling and a corresponding "hysteresis." Alternatively it may reflect a need for more flexibility in describing water dimple shape in this critical transition region. "Symmetrizing" the calculated curves suggests a significant barrier reduction (30 - 50% for q ~ 1.0e - 1.5e) relative to the classical "planar" picture. Interestingly, the barriers are reduced to ~40 kT for both q = 1.0e and q = 1.5e, while the corresponding quantities for a planar membrane are ~60 kT and 140 kT. This is a remarkable demonstration of the role played by fluctuations.

Speculations and Future Directions

- Membrane-buried charges can induce large amplitude fluctuations (dimples), poorly described by a "smectic elastic slab" model. To describe such water penetration of the lipid's hydrophobic core we modeled a "pore forming" as well as an elastic solvation mechanism.
- A cylindrical water-filled membrane-spanning pore reduces the electrostatic barrier for charge translocation several-fold. Overall energetics depends on the associated pore formation energy $W_{pore} = 2\pi\gamma R$, with γ the linear tension and R the pore radius. Estimates of γ vary widely, depending on interaction between hydrophobic bilayer organizational forces and the curvature energy due to lipid headgroup tilt attenuating the hydrophobic influences [8]. More importantly, the actual shape of the pore (its $R(z)$ dependence) must be found by optimization, much like the dimple description presented above. This analysis is in progress. More detailed description will permit analyzing cooperativity between elastic fluctuations and hydrophobic effects in charge solvation.

References

1. M. B. Partenskii et al., *Israel J. Chem.* **47**, In press (2007).
2. Long et. al., *Science*, 309, 897 (2005); *Nature*, **450,** 376 (2007).
3. G. V. Miloshevsky & P. C. Jordan, *J. Chem. Phys.* **122**, 214901 (2005).
4. Z. Zhou et al., *J. Comp. Chem.* **11,** 1344 (1996).
5. P. R. Amestoy et al., *Parallel Computing* **32**, 136 (2006).
6. http://people.brandeis.edu/~gennady/cemea.html
7. S. Dorairaj & T. W. Allen, *PNAS* **104**, 4943 (2007).
8. P. A. Bachier et al., *Biophys. J.* **92**, 4344 (2007).

email to: gennady@brandeis.edu

Acknowledgement

Work supported by a grant from the National Institutes of Health, GM-28643.